Proceedings of the 24th European Young Geotechnical Engineers Conference (EYGEC), Durham, UK
Osman, A.S. & Toll, D.G. (Eds.) 2015
ISBN 978-0-9933836-01

A fully-discrete approach to study the behavior of slope dry-stone retaining walls

J.J. Oetomo[*1], E. Vincens[2], F. Dedecker[3] and J.-C. Morel[4]

[1] *Laboratoire 3SR, UMR 5521, Grenoble, France*
[2] *University of Lyon, LTDS, UMR CNRS 5513, Ecole Centrale de Lyon, Ecully, France*
[3] *Itasca Consultants, S.A.S., Ecully, France*
[4] *University of Lyon, LTDS, UMR CNRS 5513, LGCB ENTPE, Vaulx en Velin, France*
[*] *Corresponding Author*

ABSTRACT A dry-stone retaining wall (DSRW) is a vernacular structure, built by selecting and fitting stone blocks altogether without mortar. This structure is considered as being capable of answering some challenges of sustainable development. Indeed, they use a lesser amount of embodied energy in comparison with bonded masonry or reinforced concrete structures. Nevertheless, before recently, their behavior is little known, therefore hampering the construction/rehabilitation of such walls. In this study, the behavior of DSRWs towards failure was investigated by using a discrete modeling for the three sub-systems: wall, backfill and interface. A commercial DEM package (PFC2D^{TM}) was used throughout the study. The methodology for obtaining the micromechanical parameters is described. Then, the model is validated quantitatively by comparing the numerical results with two series of full-scale experimental campaigns, where the DSRWs were loaded respectively with hydrostatic forces and backfill. In spite of its intensive simulation time, this method provides a clear insight into the structure behavior during the loading process; and being the most sophisticated modeling for such a system, it can be used as a reference to validate more simplified methods.

RÉSUMÉ Un mur de soutènement en pierre sèche (MSPS) est un ouvrage construit par assemblage de blocs rocheux sans mortier. Cette technologie est attrayante car répondant à la majorité des défis posés par le développement durable. Néanmoins, jusqu'à peu, son comportement restait peu qualifié, empêchant la construction de nouveaux murs ou la réparation de murs existants. Dans ce travail, le comportement de MSPS à la rupture est étudié par la méthode des éléments discrets. Le logiciel PFC2D^{TM} a été utilisé pour faire cette modélisation. La méthodologie pour obtenir les paramètres micromécaniques est décrite en détail. Ensuite, le modèle est validé sur la base des résultats obtenus lors de deux campagnes expérimentales sur MSPS à l'échelle 1, où les MSPS ont été chargés par, d'une part une seule charge hydrostatique et d'autre part par un remblai. En dépit du temps de calcul important nécessaire au calcul numérique, cette méthode fournit une vue claire sur le comportement du mur au cours d'un chargement. Cette méthode constitue l'approche numérique la plus sophistiquée pour ce système, elle peut être utilisée comme référence pour valider des méthodes simplifiées.

1 INTRODUCTION

The dry-stone walling was once a widely used technique, commonly found across the globe especially in mountainous region or when the stone blocks were available. Such technique has been largely overlooked since a more efficient bonded masonry and other contemporary materials (e.g. reinforced concrete) were preferred during the 20th century. Nonetheless, one survey shows that the DSRWs comprise 18% of the total retaining walls in France (Odent 2000), many built during the 19th century, while, for example, O'Reilly et al. estimated that there is around 9000 km of such walls in Great Britain (O'Reilly et al. 1999). Nowadays, many of these heritage structures are badly deteriorated.

The DSRWs are typically built with a joint inclination α and a wall batter λ_1. The wall can rise up to 10 m high (Alejano et al. 2012), but usually is found in the range of 2 to 4 m (Figure 1).

The revival of interest of DSRWs has been largely motivated by the gain of awareness of the sustainable development as the DSRWs are made with less embodied energy. Moreover, with a diffuse porosity

ranging from 20% to 45%, the water can naturally flow through the wall body; a notable advantage in comparison with the concrete retaining wall.

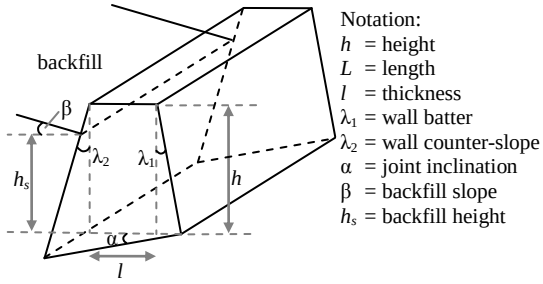

Figure 1. Geometry of a dry-stone retaining wall.

The repair and reconstruction project of damaged DSRWs are largely hampered by the lack of guidance from building standards. This can be ascribed to the complex behavior of DSRWs in which the wall might deform extensively before failure due to the block sliding. A sophisticated approach is then required to simulate this behavior in purpose of validating a simplified technique.

The failure mode of DSRWs depends on the loading applied to the structure. In the case of slope retaining wall, the wall is uniformly loaded with soils; therefore the failure mode is tied to the planar deformation mode: a sliding or toppling failure is expected. In the other hand, if the wall is also subjected to a diffused stress from a concentrated load at the top of backfill surface (e.g. from automobiles or a structure) a failure mode with true three dimensional deformations is expected. In this study, we are interested in the planar failure mode.

Recent full-scale experimental studies have been conducted by at least two groups, one from ENTPE, France (Villemus et al. 2007; Colas et al. 2010; Le 2013) and another from University of Bath, UK (Mundell et al. 2010). The numerical simulations in this paper are based on the ENTPE's studies. It consists of two series of experimental campaigns, where the DSRWs were loaded with a hydrostatic load and a backfill respectively, hereafter referred as case A and case B.

A fully discrete element method was used in this study. The calibration of the local mechanical parameters is described in detail. The results of full-scale numerical models are then compared with the published experimental results (Villemus et al. 2007; Colas et al. 2010) and the analytical study using the yield design approach (Colas et al. 2013).

Compared with classical approaches (e.g. limit equilibrium analysis, limit analysis), DEM model offers the following advantages: (1) one does not need to assume the failure mode of the DSRW as well as the slip plane of the soil; (2) the progressive failure of the DSRW can be traced.

2 EXPERIMENTAL CAMPAIGNS

The case A DSRWs were loaded with a hydrostatic load (Figure 2a). This is done by using an impervious PVC layer at the inward wall surface. In total, five walls were tested and two materials tested: limestone and schist, with a wall height ranging from 2 to 4 m. More details can be found in (Villemus et al. 2007).

In case B, four full-scale DSRWs have been built, however due to some technical difficulties, only three results are exploitable. They were built with two types of stone blocks: schist and limestone. The backfill grains were poured under gravity from a dumper, forming a natural angle of repose (Figure 2b) for the slope of 32°.

(a) (b)

Figure 2. Experimental tests of DSRWs, loaded with: (a) hydrostatic force (Villemus et al. 2007); (b) backfill (Colas et al. 2010).

These walls were backfilled with elongated-shape gravels, having diameters of 8-16 mm and a unit weight of 14.9 kN/m^3. The mechanical properties were identified by laboratory triaxial tests. For a confinement stress of 35 kPa, the backfill mechanical properties are as follows: internal friction angle ϕ_g^g = 37.7° and a dilatancy angle ψ = 8°. Find details in (Colas et al. 2010).

3 MODEL GEOMETRY

For the modeling of DSRWs, a discrete element method (Cundall & Strack 1979) has been used. The authors used a commercial DEM code, PFC2D^{TM}. This is a particle based simulation with an explicit solvation of the dynamic equations and with rigid disks as its basic element.

The dry-stone blocks are modelled as a rigid assemblage of disks. This choice was made as the wall failures in experiments were not instigated by block crushing. The disks of 8-11 mm diameter are used to create these blocks, slightly inferior to the size of backfill grains. This choice is important to obtain a representative interface roughness with the backfill.

To create the elongated grains of the backfill, rigid clumps of disks are formed. More details are given hereafter in section 5.

4 CONTACT LAWS

The interaction between disks in DEM depends on a micromechanical constitutive law, also known as contact law. In this study, two different contact laws were used. The first one is a linear contact law; it consists of a spring in both the normal and tangential direction and is formulated as follows:

$$F_n = k_n \, u_n \tag{1}$$

$$\Delta F_s = -k_s \, \Delta u_s \tag{2}$$

The sliding failure may also take place if the total compounded shear force at a contact is greater than $\mu \, F_n$, with μ the local friction angle. The normal stiffness k_n is a secant modulus, while the shear stiffness k_s is a tangent modulus. Since a high value of stiffness penalizes the computational time, this stiffness should be sufficiently low to limit it. But in the other hand, the stiffness must also be sufficiently high for the elastic behavior not to be overrepresented. Thus, a value of 5.10^7 Pa has been chosen for the normal stiffness k_n. The ratio between the normal and the tangential stiffness was taken equal to unity. This contact law is used for the contact between backfill grains and for the contact at the wall-backfill interface.

The second contact law used in this study is a smooth-joint contact law applied for contacts between blocks (Mas Ivars et al. 2008). In essence, this law is similar to the linear contact law except that the sliding failure at each contact point takes place along a same given contact direction and involves a contact area A (or line in 2D model). This law writes:

$$\Delta F_n = k_n' \, A \, u_n \tag{3}$$

$$\Delta F_s = k_s' \, A \, \Delta u_s \tag{4}$$

Based on a parametric study, the smooth-joint normal stiffness is taken equal to 10^8 Pa. The ratio between the normal and the tangential stiffness of the smooth-joint contacts was also taken equal to unity.

5 CALIBRATION OF LOCAL PARAMETERS

In order to obtain the desired global behavior, the micromechanical properties must be well calibrated for the three mechanical sub-systems of DSRWs: wall, backfill and wall-backfill interface.

5.1 Dry-stone blocks

The macro-roughness of a block-block contact is not taken into account with the usage of smooth-joint contact law. Therefore, the sliding failure between two blocks is directly dependent on the value of the micro-roughness (i.e. friction angle) of blocks.

A simulation of a tilt test has been used to validate this. Two blocks of same size were tilted progressively until failure. Figure 3 shows the kinematic of such a test. In this figure, two blocks (top block free and bottom block fixed) with a local friction angle of 30° were tilted. As observed here, the failure occurred when the global tilting angle is slightly greater than the local block friction angle, as expected.

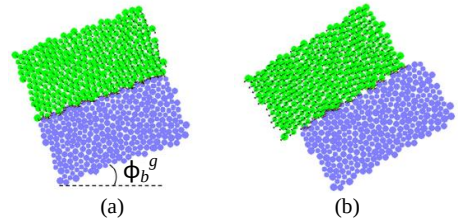

Figure 3. Kinematic of sliding failure during a tilt block test simulation with ϕ_b^l=30°: (a) ϕ_b^g=20°; (b) ϕ_b^g=31°.

5.2 Backfill

The local parameters for the backfill are identified using a series of biaxial simulations. Grains were

poured in a box of 75x150 cm^2, stabilized under the gravity, with a drop height of approximately five times the grain maximum size. A confinement pressure of 35 kPa, representative of the average site conditions, is applied.

The local parameters for grains are identified in two steps. First, we state that the backfill critical friction angle is close to the backfill natural angle of repose, i.e. 32°. Strictly speaking, this does not hold true as the critical friction angle is usually obtained with a triaxial test using a confinement pressure of 100 kPa or greater. However, as the backfill shares the same loose state, such assumption has been used.

The following parameters may influence the backfill critical friction angle: grain size, grading, grain shape and local friction angle of grains (Rothenburg & Bathurst 1992; Thornton 2000). The backfill diameter is fixed in the range of 8 to 16 mm, with a linear grading. Then, only two parameters influence the backfill critical friction angle: (1) the aspect ratio of grains; (2) the grain-grain local friction angle.

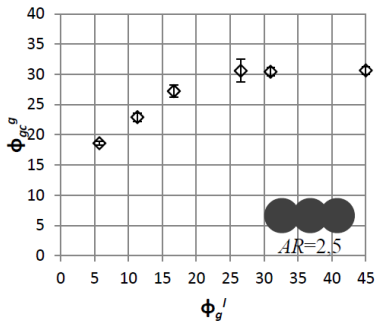

Figure 4. Backfill critical friction angle; influence of the local grain friction angle for an aspect ratio *AR* of 2.5.

A former study showed that for an aspect ratio of 1.75, the desired critical friction angle could not be greater than 27° regardless the considered local friction angle. If the aspect ratio is increased to 2.5 (Figure 4), the desired critical friction angle of 32° can be approached by using a very high value of local friction angle (e.g. ϕ_g^l = 45°). Such important value might not hold a physical meaning, however if the grain aspect ratio is further increased: (1) the interface behavior in 2D model will be dominated by local arching effects; (2) grain shape will be too elongated. Therefore, an aspect ratio of 2.5 and a local friction angle ϕ_g^l of 45° were chosen.

Finally, the backfill internal friction angle ϕ_g^g is determined in the second step. As all of the backfill local parameters have been selected, the internal friction angle ϕ_g^g depends only on the initial porosity of the sample. Figure 5 shows that the backfill internal friction angle of 37.7° can be obtained if the sample is created with an initial porosity n_0 of 0.22.

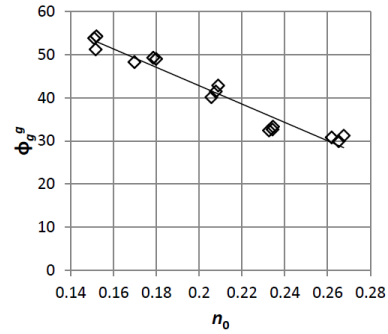

Figure 5. Backfill internal friction angle ϕ_g^g according to the sample initial porosity n_0 (*AR*=2.5 and ϕ_g^l=45°).

5.3 Backfill-wall interface

The interface is the zone in-between wall and backfill in which the shear resistance is concentrated. As both wall and backfill properties have been defined in precedent sections, the interface behavior depends only on the local friction angle between the backfill grains and the wall blocks.

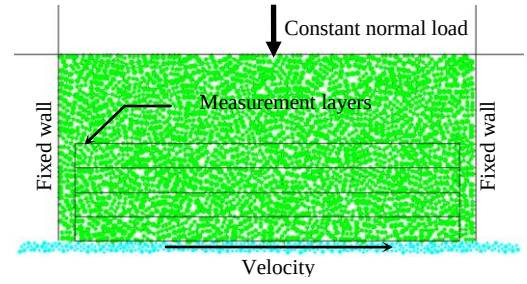

Figure 6. Simulation of an interface CNL test.

The geometrical property of interface is usually studied using the normalized roughness R_n (Kishida & Uesugi 1987), defined as a ratio of the maximal asperity of structure R_{max} and the D_{50} of backfill grains. If R_n is greater than 0.1, the interface is classified as rough, where a strain softening is observed together with some degree of dilatancy (Hu & Pu 2004). From the observation during the experimental

campaign, R_n was estimated as high as 1.5. No additional information is available. Eurocode 7 recommends that in the case of a very rough interface (e.g. case of in site concrete wall), the internal friction angle ϕ_i^g of the interface can be taken equal to the internal friction angle ϕ_g^g of the backfill. It seems relevant to extrapolate this hypothesis to the case of backfill dry stone wall interface; it was done in this study.

Figure 6 shows a DEM simulation of a typical interface Constant Normal Load (CNL) test. After the block surface is created (thin particle layer under the box), the grains are poured on the top of this surface inside a box of 90x50 cm^2. The backfill parameters described in the previous section are used herein. A constant normal load of 35 kPa is then applied at top boundary. Then, the direct shear simulation is performed by applying a constant velocity of 5.10^{-4} m/s to the bottom thin layer which is the model of the wall surface.

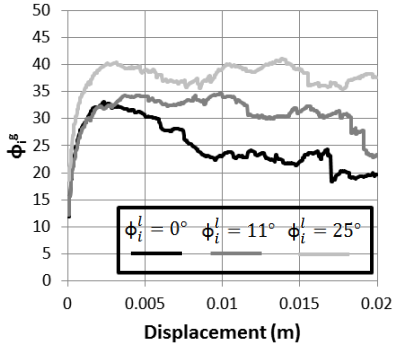

Figure 7. Evolution of the global interface friction angle according to the grain-block local friction angle.

The evolution of the interface friction angle was calculated during the simulated test inside the layers close to interface, each layer having a thickness of $3D_{50}$. The homogenization formula for calculating the shear stress is explained in-depth in (Itasca 2008). Three value of local interface friction angles have been tested (see Figure 7).

One can note that the interface geometrical roughness ($\phi_i^l = 0°$) mobilizes an important internal interface friction angle (33° at peak). Based on these tests, the desired value for ϕ_i^g of 37.7° can be attained by using a local friction angle ϕ_i^g equals to 25°.

6 NUMERICAL MODELING

The whole tests from case A and B campaigns have been modeled using the local parameters calibrated in the previous sections, where blocks in both cases were mounted in regular configuration. The foundation is modeled as a fixed layer of disks.

Two types of planar deformation failure have been observed for case A but the toppling mode of failure was only found for case B (Figure 8). The comparison between the numerical modeling with the experimental and the analytical study (yield design) by Colas et al. (Colas et al., 2013) is given in Table 1 and in Table 2 respectively. As observed in Table 2, two simulations with two random-seeds have been performed in this work. It was done to assure the reproducibility of case B simulations.

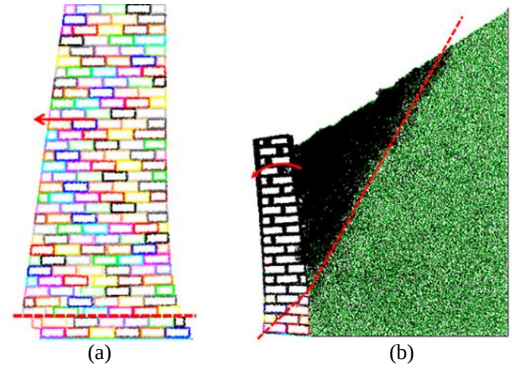

Figure 8. Failure modes of the DSRWs model: (a) sliding failure for case A; (b) toppling failure for case A and B.

For case A simulation, hydrostatic forces were applied to disks at inward face wall with approximately an increment of 1% *h* (wall height) until the wall fails. For case B, the wall was also incrementally loaded, however, in this case, with layer of grains of approximately 10 cm at a time. These grains were poured under the gravity at the right side of the backfill zone. In general, case A simulations took few hours to complete, where in the other hand a case B running needs approximately 2.5 weeks.

The case A and B simulation results show a departure of less than 9% and 7% respectively. Considering that the block arrangement and the backfilling process in experimental realizations are also a subject of a random process, hence this is a very good agreement. It appears that the omission of block

roughness has little effect on the critical height of hydrostatic load. However, it is likely to affect the wall failure mode.

CONCLUSION

A fully-discrete approach was presented in order to study the behavior of DSRWs towards failure. The process of calibration of the local mechanical parameters was readily presented. Though time consuming which is also the case for most DEM simulations, this method is the most sophisticated one to address the studied problem.

The critical loading heights observed on site were found through simulations with a high degree of precision which validates the whole approach. As a consequence, this method can be considered as a reference method to elaborate more simple approaches.

Table 1. Critical heights found through experiments, analytical approach and numerical DEM model: case A.

Wall height *h*	2.0	1.95	4.0	2.0	4.25
Wall label	V1L	V2L	V3L	V4L	V5S
Experiment	1.74*S*	1.78*T*	3.37*S*	1.90*T*	3.62*S*
Analytic (Colas et al. 2013)	1.86*S*	1.92*T*	3.74*S*	1.94*T*	3.98*S*
Relative error	7%	7%	11%	2%	11%
Numerical model (DEM)	1.89*T*	1.88*T*	3.54*S*	1.87*T*	3.77*T*
Relative error	9%	6%	5%	2%	4%

Note: values in m. *S = Sliding, T = Toppling*

Table 2. Critical heights found through experiments, analytical approach and numerical DEM model: case B.

Wall height *h* (m)	2.5	2.5	2.5
Wall label	C2S	C3S	C4L
Experiment	2.3*S*/*T*	2.78*T*	2.72*T*
Analytic (Colas et al. 2013)	2.58T	2.85T	2.67T
Relative error	12%	2%	2%
Numerical model (DEM)	(1) 2.46*T* (2) 2.38*T*	(1) 2.68*T* (2) 2.72*T*	(1) 2.53*T* (2) 2.63*T*
Relative error	(1) 7% (2) 3%	(1) 4% (2) 2%	(1) 7% (2) 3%

Note: values in m. *S = Sliding, T = Toppling*

ACKNOWLEDGEMENTS

The present work is part of the research projects C2D2 10 MGC S01 PEDRA funded by the Ministry of Ecology and RESTOR funded by the Ministry of Culture under the PNRCC program. These institutions are acknowledged for their financial support. We would like to acknowledge the Rhône-Alpes region as well for its support during this project. In relation to the EYGC, the authors would also express gratitude to CFMS and 3SR-Lab for providing the subscription and accommodation aid.

REFERENCES

Alejano, L.R. Veiga, M. Taboada, J. Díez-Farto, M. 2012. Stability of granite drystone masonry retaining walls: I. Analytical design, *Géotechnique* **62(11)**, 1013-1025.

Colas, A.S. Morel, J.C. Garnier D. 2010. Full-scale field trials to assess dry-stone retaining wall stability, *Engineering Structures* **32 (5)**, 1215-1222.

Colas, A.S. Morel, J.C. Garnier, D. 2013. Assessing the two-dimensional behaviour of drystone retaining walls by full-scale experiments and yield design simulation, *Géotechnique* **63(2)**, 107-117.

Cundall, P.A. & Strack, O.D.L. 1979. A discrete numerical model for granular assemblies, *Géotechnique* **29(1)**, 47-65.

Hu, L. & Pu, J. 2004. Testing and modeling of soil-structure interface, *Journal of geotechnical and geoenvironmental engineering*, 130 (8), 851-860.

Itasca Consulting Group Inc. 2008. Particle Flow Code in 2 Dimensions: Theory and Background, Fourth Edition. Itasca: Minnesota.

Kishida, H. & Uesugi, M. 1987. Tests of the interface between sand and steel in the simple shear apparatus, *Géotechnique* **37(1)**, 45-52.

Le, H.H. 2013. Stabilité des murs de soutènement routiers en pierre sèche : Modélisation 3D par le calcul à la rupture et expérimentation échelle 1, *PhD Thesis*.

Mas Ivars, D. Potyondy, D. Pierce, M. Cundall, P. 2008. The smooth-joint contact model. *In: Proceedings of the 8th World Congress on Computational Mechanics and 5th European Congress on Computational Methods in Applied Sciences and Engineering*, Venice, Italy. Paper No. a2735.

Mundell, C. McCombie, P. Heath, A. Harkness, J. Walker, P. 2010. Behaviour of drystone retaining structures, *Proceedings of the ICE – Structures and Buildings* **163(1)**, 3-12.

Odent, N. 2000. Recensement des ouvrages de soutènement en bordure du réseau routier national, *Ouvrages d'art - centre des techniques d'ouvrages d'art* **34**, 15-18.

O'Reilly, M.P. Bush, D.I. Brady K.C., Powrie W. 1999. The stability of drystone retaining walls on highways, *Proceedings of the ICE - Municipal Engineer* **133(2)**, 101-107.

Rothenburg, L & Bathurst, R.J. 1992. Micromechanical features of granular assemblies with planar elliptical particles, *Géotechnique* **42(1)**, 79-95.

Villemus, B. Morel, J.C. Boutin, C. 2007. Experimental assessment of dry stone retaining wall stability on a rigid foundation, *Engineering Structures* **29(9)**, 2124-2132.

Thornton, C. 2000. Numerical simulations of deviatoric shear deformation of granular media, *Géotechnique* **50(1)**, 43-53.